EUKARYOTIC CELL, Apr. 2011, p. 611–615 Vol. 10, No. 4
1535-9778/11/$12.00 doi:10.1128/EC.00315-10

NOTE

Regulatable Ras Activity Is Critical for Proper Establishment and Maintenance of Polarity in *Aspergillus fumigatus*▽†

Jarrod R. Fortwendel,[1,2] Praveen R. Juvvadi,[1] Luise E. Rogg,[1] and William J. Steinbach[1,2]*

Department of Pediatrics, Division of Pediatric Infectious Diseases, Duke University Medical Center, Durham, North Carolina,[1] and Department of Molecular Genetics and Microbiology, Duke University Medical Center, Durham, North Carolina[2]

Received 14 December 2010/Accepted 24 January 2011

Here we show that expression of a constitutively activated RasA allele, as the sole source of Ras activity, revealed novel Ras-induced phenotypes, including excessive vacuolar expansion and spontaneous lysis of hyphal compartments. These findings highlight the requirement for balanced Ras activity in the establishment and maintenance of polarized growth in filamentous fungi.

The *Aspergillus fumigatus rasA* gene is a major regulator of hyphal morphogenesis (6, 8). Although nonessential in the yeast-like fungi *Saccharomyces cerevisiae* (13), *Schizosaccharomyces pombe* (9), *Candida albicans* (5), and *Cryptococcus neoformans* (1), deletion of the RasA homolog is lethal in the filamentous fungi *Aspergillus nidulans* (18), *Penicillium marneffei* (3), and *Colletotrichum trifolii* (10, 19). Due to the essential nature of the RasA homologs in many filamentous fungi, mechanistic studies have required expression of either a constitutively active or an inactive RasA mutant in a wild-type background. Data generated in this manner for *P. marneffei*, *A. fumigatus*, *A. nidulans*, and *C. triffolii* have revealed a conserved role for Ras in polarized morphogenesis and asexual development of filamentous fungi (3, 8, 18, 19). However, the requirement for nonphysiological expression of the mutant Ras locus, as well as the presence of the wild-type Ras allele, may obscure some phenotypes caused by constitutive activation of the Ras protein. Here, we sought to more clearly define the effects of deregulated RasA activity on polarized growth and morphogenesis of filamentous fungi by utilizing the viable *A. fumigatus* Δ*rasA* mutant. To generate an *A. fumigatus* strain with completely deregulated RasA activity, we cloned a mutant *rasA* allele cDNA with a glycine-to-valine substitution at amino acid position 17 (G17V) into expression vector pARPh. The G17V mutation is predicted to result in a dominant active RasA protein. Vector pARPh contains a 1.5-kb fragment of the *rasA* endogenous promoter followed by the *nos* terminator from vector pUCGH (12) and a 1.5-kb phleomycin resistance cassette (17). We then transformed this construct into the Δ*rasA* background. Transformants were isolated on phleomycin-containing medium, and single integration of the transforming plasmid was confirmed by Southern analysis (data not shown). Five separate transformants, each derived from an ectopic integration event, were recovered and found to have similar phenotypes. The results described herein represent one representative strain. The interpretation of data generated using the DA*rasA1* strain, expressing constitutively active RasA as the only source of RasA activity, will not be complicated by the presence of a wild-type *rasA* locus.

Our previous studies with *A. fumigatus* showed that the simultaneous expression of the wild-type RasA allele and an activated RasA allele led to delayed conidiophore formation, whereas hyphal development was normal (8). To examine the impact of completely deregulated Ras activity, we compared colony growth and morphology of the original *A. fumigatus* DA*rasA* mutant (8) with those of the newly generated DA*rasA1* mutant. In contrast to the DA*rasA* mutant, the DA*rasA1* strain displayed compact colony morphology similar to that of the Δ*rasA* mutant (Fig. 1A). After 72 h of growth on minimal medium, the colony diameter of the DA*rasA1* mutant (12.3 ± 0.6 mm) was only slightly larger than that of Δ*rasA* (10.2 ± 0.3 mm). In comparison, the DA*rasA* mutant (37.3 ± 1.5 mm) displayed a final colony diameter similar to that of the wild type (37.2 ± 0.8 mm) (Fig. 1B). Although the colony diameter differences between the DA*rasA1* and Δ*rasA* mutants were statistically significant ($P < 0.01$) for all five DA*rasA1* isolates, these data imply that deletion and complete deregulation of RasA cause similar inhibitions of radial growth. In similarity to previously reported data for the DA*rasA* mutant (8), conidiophore development of the DA*rasA1* strain was delayed, requiring 72 h of culture for full development versus the 24 h required for the wild type. The morphology of DA*rasA1* conidiophores was also aberrant, with large, misshapen vesicles and shortened phialides (see Fig. S1 in the supplemental material). Taken together, these results suggested that the underlying wild-type RasA allele did affect phenotypic outcome in the DA*rasA* strain and prompted further investigation of DA*rasA1*. Upon microscopic evaluation, the DA*rasA1* mutant was found to have severely delayed polarity establishment, as characterized by hyperswollen conidia (Fig. 1C). After 12 h of incubation, DA*rasA1* conidia displayed only 46% germination

* Corresponding author. Mailing address: Department of Pediatrics, Division of Pediatric Infectious Diseases, 427 Jones Building, Duke University Medical Center, Durham, NC 27710. Phone: (919) 681-1504. Fax: (919) 668-4859. E-mail: stein022@mc.duke.edu.

† Supplemental material for this article may be found at http://ec.asm.org/.

▽ Published ahead of print on 28 January 2011.

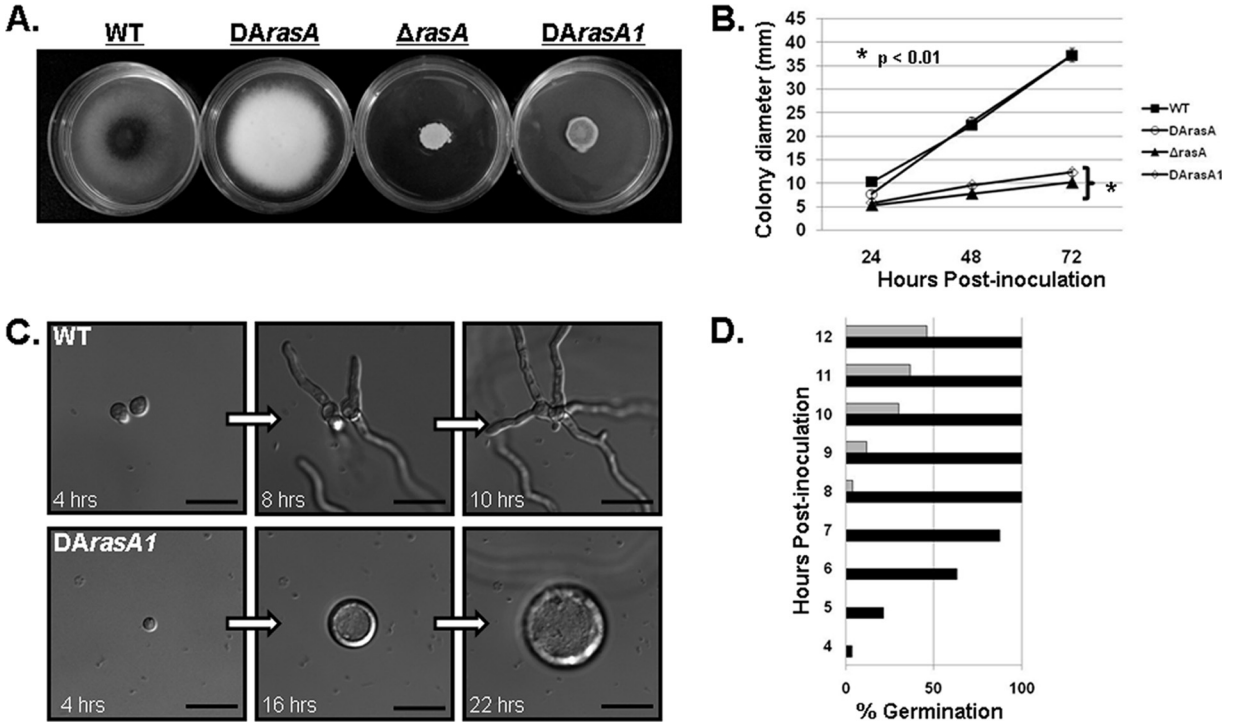

FIG. 1. Dergulated Ras causes decreased growth and delayed polarity establishment. (A) Colony morphology comparison of the wild-type (WT), Δ*rasA*, DA*rasA*, and DA*rasA1* strains. Note the striking differences in colony morphologies of the DA*rasA* mutant (activated Ras in a wild-type background) compared to those of the DA*rasA1* mutant (activated Ras in the Δ*rasA* background). A total of 10,000 conidia were inoculated onto minimal media and incubated for 72 h at 37°C. (B) Quantification of the average colony diameter for each strain at 24, 48, and 72 h postinoculation. Statistical analysis (Student's *t* test) of triplicate samples was performed for the Δ*rasA* and DA*rasA1* strain at 72 h. (C) Comparison of germination of WT versus DA*rasA1* strains. Note the extended time course and complete block of polarity establishment in the DA*rasA1* strain. (D) Quantitative analysis of germ tube emergence of the WT (black bar) and DA*rasA1* (gray bar) strains over the first 12 h of incubation at 37°C.

(Fig. 1D). A small proportion of the DA*rasA1* conidia never produced a polarized growth axis (data not shown). These data are in contrast to the results seen with the wild-type strain, which germinated completely within 8 h (Fig. 1C and D).

In a wild-type genetic background, expression of activated RasA causes an increase in nuclear content during the initial stages of germination (8). Similarly, nuclear staining of the DA*rasA1* mutant revealed increased nuclear content during germination, although this was associated with an exaggerated isotropic growth phase (Fig. 2A, panel ii). Even though the germinating DA*rasA1* conidium was hyperswollen and multinucleated, initial DA*rasA1* germ tubes exhibited hyphal volume, septation, and nuclear distribution that were indistinguishable from the wild-type results (Fig. 2A, panels i through iv). However, once the fully polarized hyphae were growing, subapical compartments of the DA*rasA1* mutant displayed an increased hyphal compartment volume and contained many nuclei (Fig. 2A, panel v). This suggests that, rather than undergoing septation and entering quiescence, subapical compartments of the DA*rasA1* mutant reinitiated an isotropic phase and continued nuclear division. In addition, a proportion of DA*rasA1* germ tubes appeared to represent abortive growth axes, displaying a swollen hyphal tip (Fig. 2A, panel vi). To clearly delineate the temporal presentation of the DA*rasA1* morphological abnormalities, we utilized live-cell microscopy analysis of the wild-type and DA*rasA1* strains. Upon evaluation, the delayed polarity establishment and exaggerated isotropic growth of the DA*rasA1* mutant were found to be accompanied by accumulation of many vacuoles of various sizes in the initial conidium (see movie S1 in the supplemental material). Each germinating DA*rasA1* conidiospore developed a single, large central vacuole that persisted within the swollen conidium as well as multiple, smaller vacuoles that migrated into the nascent germ tube as germination began (see movie S1 in the supplemental material). After polarity establishment, large vacuoles continued to expand within the swollen subapical compartments of the DA*rasA1* mutant (Fig. 2B, panel iii; see also movie S2 in the supplemental material). Although vacuolar accumulation and expansion were apparent in subapical compartments of the wild type (see movie S3 in the supplemental material), this process was overtly aberrant in the DA*rasA1* mutant. Live-cell analysis also confirmed the presence of abortive growth axes and subapical hyphal compartments that underwent excessive swelling and vacuolization (see movie S2 in the supplemental material). Surprisingly, three separate lysis events were recorded within a single germinating DA*rasA1* conidium, two from an aborted axis and one from a subapical compartment of an actively polarized hypha (Fig. 2B, panels iv to vi; see also movie S2 in the supplemental material). Immediately following the first lysis event, the development of an intrahyphal hypha was observed (see movie S2 in the supplemental material). These findings were indicative of a po-

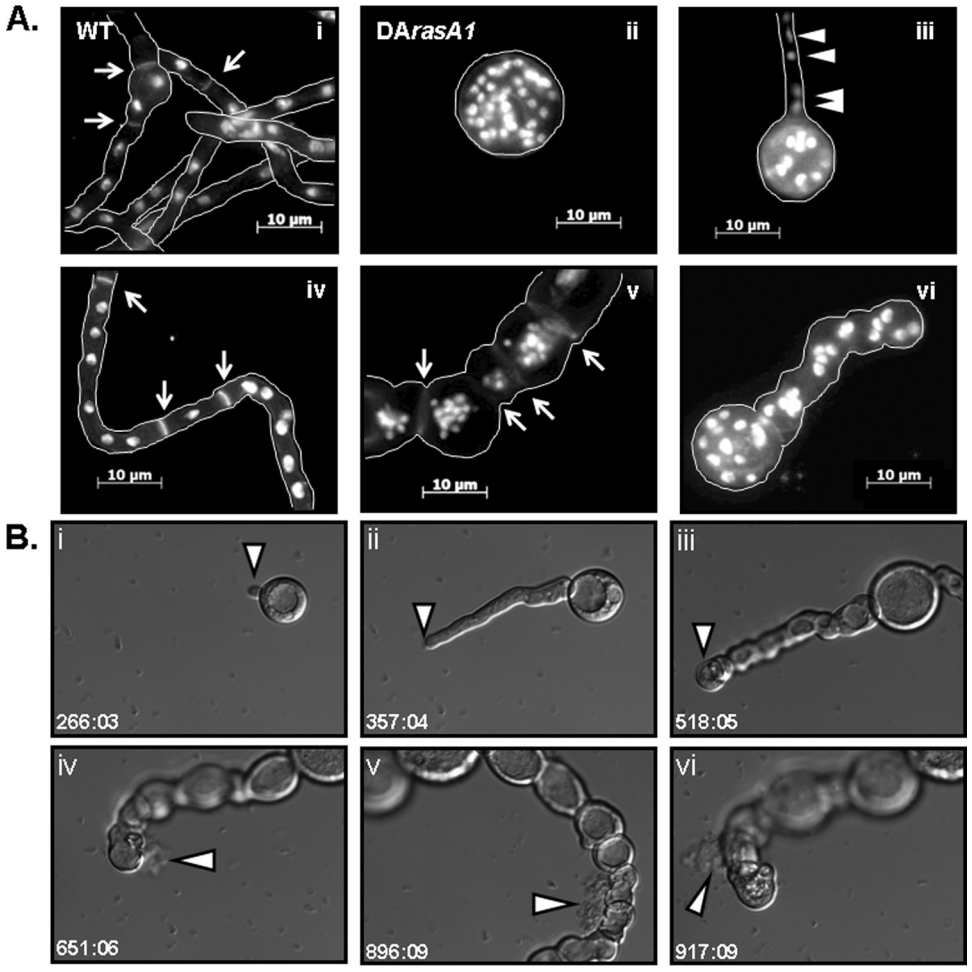

FIG. 2. DA*rasA1* expression causes loss of polarized growth axes, hyphal swelling, vacuolization, and spontaneous lysis. (A) The wild-type (WT) and DA*rasA1* strains were grown for 12 h and stained with calcofluor white (CFW) and propidium iodide (PI) to visualize the cell wall and nuclei, respectively. Staining and microscopy were performed as previously described (4). (Panel i) Wild-type *A.fumigatus*, displaying a normal distribution of nuclei throughout the hyphae and accompanied by minimal swelling of the initial conidiospore (arrows denote septa). (Panel ii) Hyperswollen DA*rasA1* conidiospore with increased nuclear content. (Panel iii) Nascent DA*rasA1* germling, showing normal distribution of nuclei (arrowheads) along the germ tube. (Panel iv) DArasA1 hyphae with normal nuclear distribution among hyphal compartments delineated by septa (arrows). (Panel v) Mature DA*rasA1* hyphae with swollen subapical compartments and increased nuclear content (arrows denote septa). (Panel vi) Aborted polarized growth axes in the DA*rasA1* mutant with swollen germ tube. (B) Conidia of strain DA*rasA1* were preincubated in glucose minimal medium (GMM) at 37°C for 4 h in 6-well, glass-bottom tissue culture plates. Following preincubation, plates were used for live-cell analysis performed with an Inverted Zeiss Axio Observer microscope equipped with a 37°C environmental chamber. The time stamp values displayed for live-cell movies and still-frame images represent minutes:seconds of the postpreincubation period. The scale bar displayed in the live-cell movies in the supplemental material represents 50 μM. (Panels i to iii) Still-frame images of a DA*rasA1* abortive-growth axis from movie S2 in the supplemental material. The arrowheads follow the position of the hyphal tip, which ceased polarized extension after the time point represented by panel ii and reentered isotropic growth coupled with vacuolar expansion, as shown in panel iii. (Panels iv to vi) Still-frame images of spontaneous lysis of hyphal compartments (arrowheads) in the DA*rasA1* strain from movie S2 in the supplemental material. Arrowheads indicate ruptured compartments with released cellular debris.

tential cell wall integrity defect in the DA*rasA1* mutant. However, growth under a variety of conditions commonly used to ameliorate hyphal swelling due to cell wall defects did not remediate growth (see Fig. S2 in the supplemental material). This likely indicates that the swelling and lysis events observed for DA*rasA1* were not due to an overt cell wall defect.

Because complete deregulation of RasA via expression of DA*rasA1* caused severe growth abnormalities, we reasoned that an increase in the wild-type RasA gene dosage might also be detrimental to growth. An increase in intracellular RasA protein levels would presumably lead to increased, albeit regulatable, RasA activity. To achieve increased RasA levels, we generated mutants in the Δ*rasA* background, expressing RasA from the constitutive *otef* promoter taken from vector pUCGH (12). Southern blot analysis was used to identify transformants with single and multiple integration events (data not shown). Two separate transformants containing a single integration of the pOtef-RasA cassette exhibited an ~9-fold increase in transcriptional levels by reverse transcription-PCR (RT-PCR) and displayed reduced conidiation and an increased radial growth rate compared to wild-type results (0.6 ± 0.03 mm/h versus 0.4 ± 0.06 mm/h, respectively). These data suggest that a

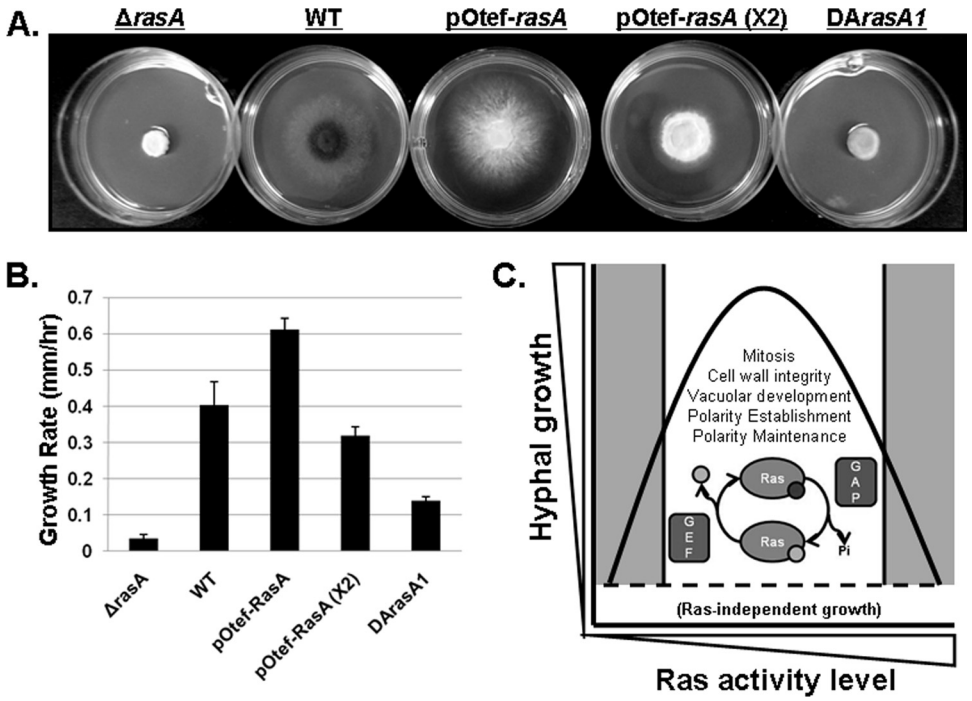

FIG. 3. Increased *rasA* gene dosage or deregulation of *rasA* gene product causes reduced radial outgrowth. (A) Comparison of colony morphologies of the Δ*rasA*, WT, pOtef-RasA (with a single integration of the pOtef-RasA cassette), pOtef-RasA (X2) (with two integrations of the pOtef-RasA cassette), and DA*rasA1* strains. (B) Quantitative comparison of the growth rates of each strain at 48 and 72 h of incubation. Growth rate determinations were performed in triplicate for all strains. Columns and error bars represent the means ± standard deviations, respectively. (C) Model representing hyphal outgrowth as a function of RasA activity in *A. fumigatus*. Gray-colored areas represent extreme inhibition or deregulation of RasA activity. Cellular processes regulated by Ras activity that affect hyphal morphogenesis are listed under the hyphal growth curve. GEF, guanine exchange factor; GAP, GTPase-activating protein.

moderate increase in regulatable RasA activity may actually enhance polarized growth (Fig. 3A and B). However, integration of two copies of the pOtef-RasA cassette, leading to an ~50-fold increase in *rasA* transcriptional levels, caused a significantly decreased growth rate (0.3 ± 0.02 mm/h) compared to wild-type results (Fig. 3A and B). As noted earlier, complete deregulation of RasA (DA*rasA1*) caused a growth rate similar to that of the Δ*rasA* mutant (Fig. 3A and B). Although RT-PCR analysis revealed a wide range of RasA expression levels for the five DA*rasA1* transformants (5- to 15-fold increases compared to wild-type results), the phenotypes of each strain were the same. This suggests that the phenotypic differences between the DA*rasA* and DA*rasA1* mutants were not likely due to activated RasA expression-level differences but to the presence of activated RasA as the sole source of Ras activity. These findings suggest that Ras pathways contribute to hyphal growth in a manner that requires a delicate balance with respect to regulated Ras signaling. Therefore, polarized morphogenesis in *A. fumigatus* can be viewed as a function of regulatable RasA activity, where too much or too little activation of the Ras protein negatively affects hyphal growth (Fig. 3C). Properly regulated Ras is hypothesized to control the orchestration of cellular processes that, in turn, support the sustained polarized growth lifestyle of filamentous fungi. Our data, along with studies from other groups (6–8, 11, 15, 18), have identified some of the cellular processes controlled by Ras activity, such as the establishment and maintenance of polarity, initiation of mitosis followed by quiescence after septation, maintenance of cell wall integrity, and vacuolar expansion.

Although some similarities persist between the DA*rasA* and DA*rasA1* mutants, the results presented here show that expression of activated RasA as the sole source of Ras activity revealed novel phenotypic changes that were not evident when activated RasA is expressed in the wild-type background. The cellular changes induced in the DA*rasA1* strain confirm earlier work with *A. nidulans* showing that increased RasA activity causes cessation of growth throughout the developmental life cycle (15, 18). Our data also coincide with a more recent report of the role of GapA, a GTPase-activating protein (GAP), in hyphal morphogenesis of *A. nidulans* (11). Deletion of *gapA*, the putative GAP for *A. nidulans* RasA, causes reduced radial outgrowth, delayed polarity establishment, and abortive growth axes (11). As GapA is hypothesized to downregulate RasA by increasing the rate of GTP hydrolysis, these outcomes are likely due to increased intracellular RasA activity. Despite these similarities, the DA*rasA1* strain has also revealed new phenotypes, including excessive vacuolar expansion and spontaneous lysis of hyphal compartments, elucidating new roles for Ras activity in polarized growth and morphogenesis.

Recently, a new form of cell death, termed "methuosis," was described for glioblastoma cells (16). Methuosis is distinct from apoptotic- and necrotic-cell death and is caused by Ras-mediated upregulation of macropinocytosis coupled with inhibition of proper endocytic membrane recycling (16). The cel-

lular changes leading to methuotic cell death, namely, excessive vacuolization and cell lysis, are strikingly similar to those reported here for the DA*rasA1* mutant. In addition, methuosis is driven by deregulated activation of the downstream Ras effector, Rac1, and the subsequent downregulation of Arf6, a protein controlling endocytic vesicle recycling (2). Mutations that constitutively activate RacA, the homolog of human Rac1, in *A. fumigatus* have not been reported. However, constitutive activation of Rac in *C. trifolii* causes vacuolated hyphal swellings reminiscent of the morphological changes in the DA*rasA1* mutant noted here (4). The *A. nidulans* homolog of Arf6, *arfB*, was recently deleted and was subsequently shown to play a conserved role in fungal endocytosis (14). The *A. nidulans* Δ*arfB* mutant also displays some phenotypes similar to those of our DA*rasA1* strain, including delayed polarity establishment marked by swollen, multinucleated conidia (14). When considered with these recent findings, our data support the hypothesis that Ras may control polarity establishment and maintenance in filamentous fungi, at least in part, through the regulation of a homologous pathway. Since both the inhibition and deregulation of Ras-controlled pathways are severely detrimental to polarized growth, the potential conservation of a Ras-mediated methuosis pathway in *A. fumigatus* may eventually have therapeutic implications. Future work is planned to focus on elucidating Ras-mediated control of endocytosis and the roles of RacA and ArfB in this process.

We thank J. Andrew Alspaugh and Connie B. Nichols for critical reading of the manuscript.

This work was supported by the Molecular Mycology and Pathogenesis Training Program at Duke University (grant 5T32-AI052080 to J.R.F.) and by a Children's Miracle Network grant and a Basic Science Faculty Development grant from the American Society for Transplantation to W.J.S.

REFERENCES

1. **Alspaugh, J. A., L. M. Cavallo, J. R. Perfect, and J. Heitman.** 2000. RAS1 regulates filamentation, mating and growth at high temperature of *Cryptococcus neoformans*. Mol. Microbiol. **36:**352–365.
2. **Bhanot, H., A. M. Young, J. H. Overmeyer, and W. A. Maltese.** 2010. Induction of nonapoptotic cell death by activated Ras requires inverse regulation of Rac1 and Arf6. Mol. Cancer Res. **8:**1358–1374.
3. **Boyce, K. J., M. J. Hynes, and A. Andrianopoulos.** 2005. The Ras and Rho GTPases genetically interact to co-ordinately regulate cell polarity during development in *Penicillium marneffei*. Mol. Microbiol. **55:**1487–1501.
4. **Chen, C., and M. B. Dickman.** 2004. Dominant active Rac and dominant negative Rac revert the dominant active Ras phenotype in *Colletotrichum trifolii* by distinct signalling pathways. Mol. Microbiol. **51:**1493–1507.
5. **Feng, Q., E. Summers, B. Guo, and G. Fink.** 1999. Ras signaling is required for serum-induced hyphal differentiation in *Candida albicans*. J. Bacteriol. **181:**6339–6346.
6. **Fortwendel, J. R., et al.** 2008. *Aspergillus fumigatus* RasA regulates asexual development and cell wall integrity. Eukaryot. Cell **7:**1530–1539.
7. **Fortwendel, J. R., et al.** 2009. Differential effects of inhibiting chitin and 1,3-β-D-glucan synthesis in Ras and calcineurin mutants of *Aspergillus fumigatus*. Antimicrob. Agents Chemother. **53:**476–482.
8. **Fortwendel, J. R., J. C. Panepinto, A. E. Seitz, D. S. Askew, and J. C. Rhodes.** 2004. *Aspergillus fumigatus rasA* and *rasB* regulate the timing and morphology of asexual development. Fungal Genet. Biol. **41:**129–139.
9. **Fukui, Y., T. Kozasa, Y. Kaziro, T. Takeda, and M. Yamamoto.** 1986. Role of a ras homolog in the life cycle of *Schizosaccharomyces pombe*. Cell **44:** 329–336.
10. **Ha, Y.-S., S. D. Memmott, and M. B. Dickman.** 2003. Functional analysis of Ras in *Colletotrichum trifolii*. FEMS Microbiol. Lett. **226:**315–321.
11. **Harispe, L., C. Portela, C. Scazzocchio, M. A. Penalva, and L. Gorfinkiel.** 2008. Ras GTPase-activating protein regulation of actin cytoskeleton and hyphal polarity in *Aspergillus nidulans*. Eukaryot. Cell **7:**141–153.
12. **Juvvadi, P. R., et al.** 2008. Calcineurin localizes to the hyphal septum in *Aspergillus fumigatus*: implications for septum formation and conidiophore development. Eukaryot. Cell **7:**1606–1610.
13. **Kataoka, T., et al.** 1984. Genetic analysis of yeast RAS1 and RAS2 genes. Cell **37:**437–445.
14. **Lee, S. C., S. N. Schmidtke, L. J. Dangott, and B. D. Shaw.** 2008. *Aspergillus nidulans* ArfB plays a role in endocytosis and polarized growth. Eukaryot. Cell **7:**1278–1288.
15. **Osherov, N., and G. May.** 2000. Conidial germination in *Aspergillus nidulans* requires RAS signaling and protein synthesis. Genetics **155:**647–656.
16. **Overmeyer, J. H., A. Kaul, E. E. Johnson, and W. A. Maltese.** 2008. Active Ras triggers death in glioblastoma cells through hyperstimulation of macropinocytosis. Mol. Cancer Res. **6:**965–977.
17. **Richie, D. L., et al.** 2009. A role for the unfolded protein response (UPR) in virulence and antifungal susceptibility in *Aspergillus fumigatus*. PLoS Pathog. **5:**e1000258.
18. **Som, T., and V. S. Kolaparthi.** 1994. Developmental decisions in *Aspergillus nidulans* are modulated by Ras activity. Mol. Cell. Biol. **14:**5333–5348.
19. **Truesdell, G. M., C. Jones, T. Holt, G. Henderson, and M. B. Dickman.** 1999. A Ras protein from a phytopathogenic fungus causes defects in hyphal growth polarity, and induces tumors in mice. Mol. Gen. Genet. **262:**46–54.